Headline Articles

4,7,11,14,18,21-Hexa-*t*-butyltribenzodecacyclenyl Radical: A Six-Stage Amphoteric Redox System[1]

Takashi Kubo,* Kagetoshi Yamamoto,* Kazuhiro Nakasuji,* Takeji Takui,† and Ichiro Murata††

Department of Chemistry, Graduate School of Science, Osaka University, Toyonaka, Osaka 560-0043

†Department of Chemistry, Faculty of Science, Osaka City University, Sumiyoshi-ku, Osaka 558-8585

††Fukui Institute of Technology, Gakuen, Fukui 910-8505

(Received May 1, 2001)

A six-stage amphoteric redox hydrocarbon radical **3**• containing three phenalenyl units was prepared. Cyclic voltammogram of **3**• exhibits six reversible redox waves with a small numerical sum (E_1^{sum}) of first oxidation (E_1^{ox}) and reduction (E_1^{red}) potentials. Some redox states of **3**• were successfully generated from the neutral **3**• and characterized by NMR, ESR, UV-vis-NIR spectroscopies, and theoretical calculations. The spin and the charges are delocalized over the entire C_3 molecule of $\mathbf{3}^{3+}$, $\mathbf{3}^{\bullet 2+}$, **3**•, and $\mathbf{3}^{3-}$. On the other hand, $\mathbf{3}^{\bullet 2-}$ shows the localization of the spin on one phenalenyl unit; these results are consistent with the distorted C_2 structure caused by the Jahn-Teller effect.

Multi-stage amphoteric redox compounds have been subject to extensive investigation.[2] These compounds show some important features: 1) their high redox abilities, which are characterized by the numerical sum (E^{sum}) of oxidation (E^{ox}) and reduction potential (E^{red}), and 2) stability of the redox species generated by multi-stage electron transfer. In these chemistries, phenalenyl structures play an important role to develop amphoteric redox properties. Recently, *s*-indaceno[1,2,3-*cd*:5,6,7-*c*′*d*′]-diphenalene (IDPL)[2f,2g] derivatives and pentaleno[1,2,3-*cd*:4,5,6-*c*′*d*′]diphenalene (PDPL)[2e] containing two phenalenyl units have been synthesized and characterized by NMR, ESR, UV/vis/NIR, and cyclic voltammetry. IDPLs and PDPL exhibited small E_1^{sum} values and gave stable redox species. These compounds are designed so that the unstable *s*-indacene and pentalene structures in the neutral states disappear in the oxidation and reduction states. This should lead to a small difference in the thermodynamic potentials between the neutral and the redox states.

On the other hand, open-shell compounds are also potential candidates for redox systems. On the basis of the simple HMO theory, the magnitudes of electron affinities and ionization potentials for open-shell species are equal, i.e., $E^{sum} = 0$. Thus, open-shell compounds should intrinsically exhibit small E^{sum} values. For example, phenalenyl radical shows quite a small E_1^{sum} (1.6 V) compared to closed-shell compounds with similar ring size.[3]

As a target compound to study properties of amphoteric open-shell hydrocarbons, we designed tribenzodecacyclenyl radical **1**• containing three phenalenyl units (Chart 1).

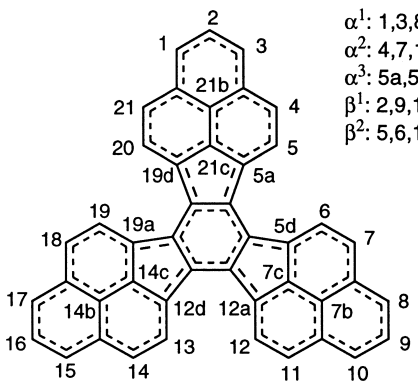

Tribenzodecacyclenyl **1**

Chart 1.

The simple HMO calculations give insight into the redox properties of **1**• (Fig. 1). The molecular orbitals ψ_{22}, ψ_{23}, and ψ_{24} correspond to the frontier orbitals of **1**•. The small energy gap between ψ_{22} and ψ_{24} suggests the small E^{sum} values and easy generation of redox species from trication $\mathbf{1}^{3+}$ to trianion $\mathbf{1}^{3-}$. Thus, **1**• is expected to behave as a six-stage amphoteric redox compound (Fig. 2). We describe here the synthesis and amphoteric redox properties of **1**• investigated by spectroscopic and electrochemical methods.

Results and Discussion

Synthesis. An attempt to isolate the parent **1**• failed due to

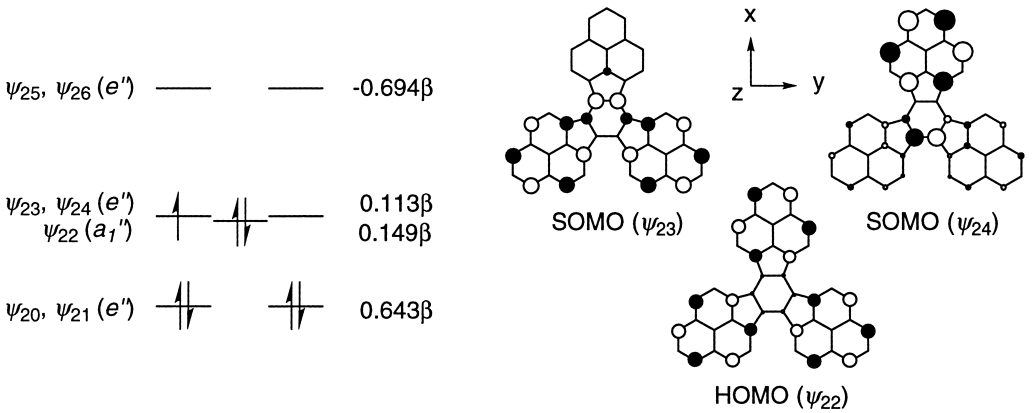

Fig. 1. Selected molecular orbitals of **1**• calculated by the HMO method.

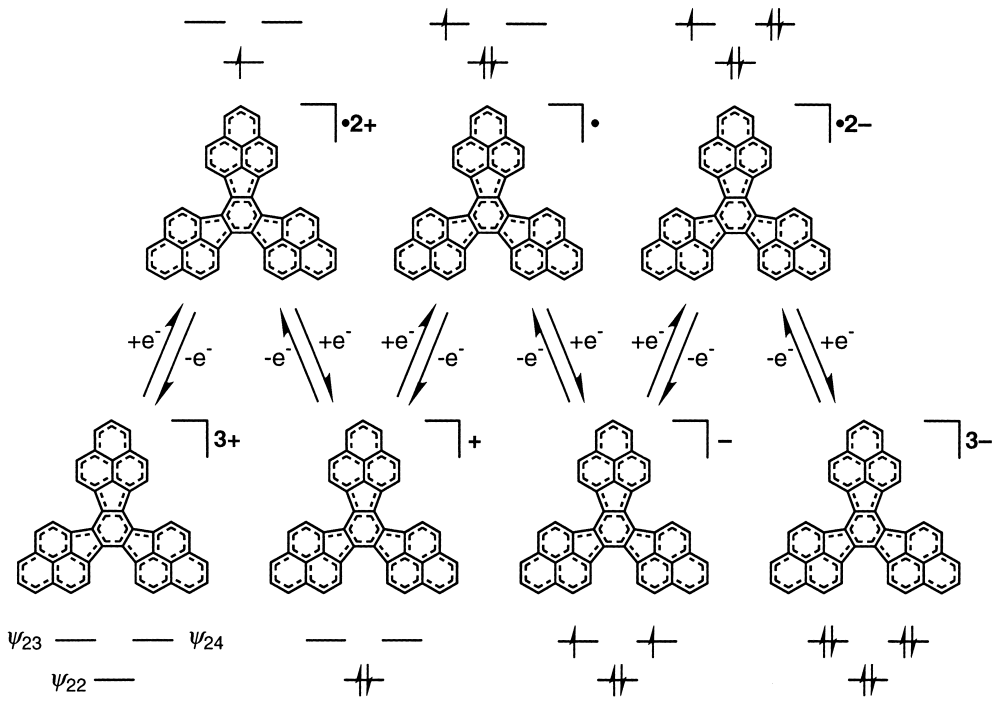

Fig. 2. Six-stage amphoteric redox behavior of **1**•.

its low solubility and instability. In order to increase the solubility, simple alkyl substituents were introduced at the β-positions of phenalenyl units of **1**•. Because the carbons at β-positions bear small LCAO coefficients in the frontier orbital, the parent compound will be only slightly perturbed by the alkyl substitution. Although tri-*n*-propyl derivative **2**• increased solubility, **2**• was found to be air-sensitive. The instability of **2**• prevented further investigations of the properties for a six-stage amphoteric redox compound. The failure to characterize the unsubstituted and β-substituted tribenzodecacyclenyl species forced us to introduce substituents at the α-positions of the phenalenyl units.

As the target of our efforts, we prepared the symmetrical 4,7,11,14,18,21-hexa-*t*-butyltribenzodecacyclenyl radical **3**• from commercially available decacyclene following Scheme 1, similar to the previously developed in the synthesis of IDPLs, PDPL, and phenalene.

Firstly, six *t*-butyl groups were introduced at the β-position of the naphthalene units of decacyclene. *t*-Butylation of decacyclene with equimolar $AlCl_3$ and a large excess of *t*-butyl chloride afforded successfully 2,5,8,11,14,17-hexa-*t*-butyldecacyclene **4** as yellow needles in 74% yield. Subsequent bromination in dichloromethane at room temperature afforded tribromide **5** in 76% yield as an isomeric mixture. Two regioisomeric tribromides could not be separated by column chromatography or recrystallization. However, the difficult separation of these compounds did not disturb our plan, because they were converted to single symmetrical products in the final steps: **11** to **3**•, and **11** to $\mathbf{3}^{3-}$, respectively. The lithiation of **5** with *n*-BuLi and subsequent methylation with MeI in THF afforded compounds **6** with trimethyl groups in 81% yield. The reaction in DME instead of THF gave considerable amounts of mono- and di-methyl derivatives. Benzylic bromination of **6** with NBS and a catalytic amount of dibenzoyl peroxide gave

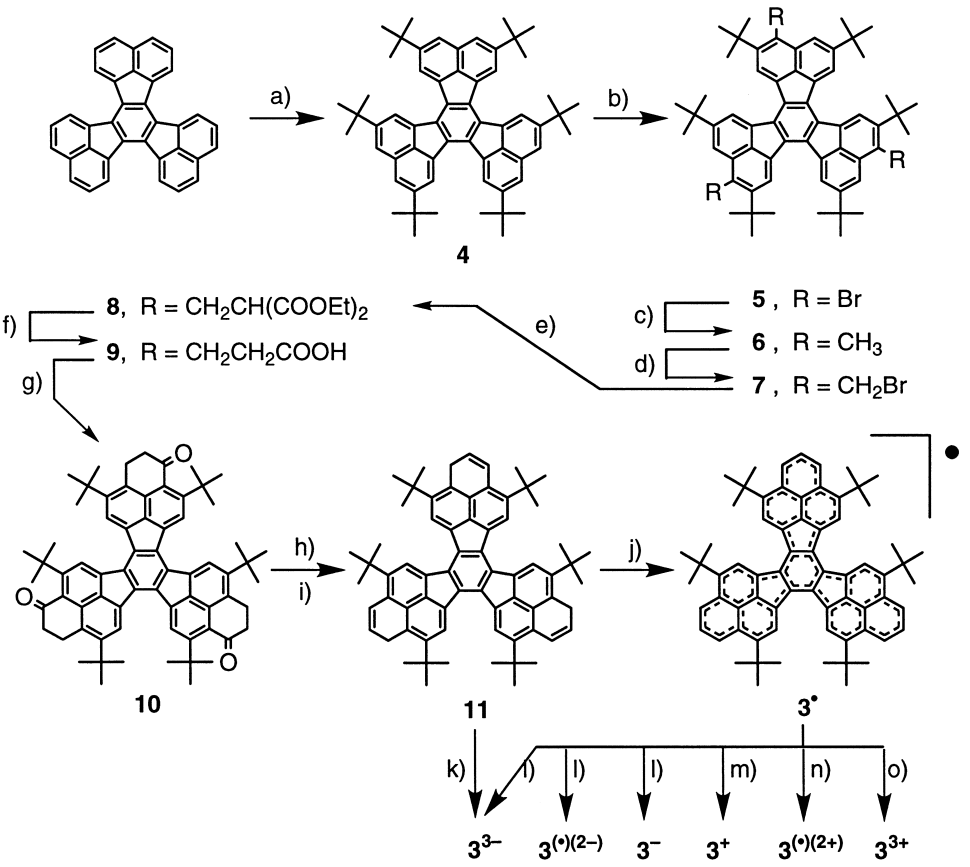

Reaction conditions : a) *t*BuCl, $AlCl_3$, CH_2Cl_2, rt, 2 h, 74% . b) Br_2, CH_2Cl_2, 2 h, rt, 76%. c) *n*BuLi, CH_3I, THF, -78 ˚C to rt, 81%. d) NBS, benzoyl peroxide, benzene, reflux, 10 min, 96%. e) NaOEt, $CH_2(CO_2Et)_2$, benzene + ethanol, rt, 1 d, 36%. f) 1) aqueous KOH, EtOH, 2) 4 N HCl, 3) 100 ˚C, 95%. g) 1) $(COCl)_2$, 2) $AlCl_3$, CH_2Cl_2, -50 ˚C, 4 h, 99%. h) LAH, THF, rt, 2 h, 77%. i) cat. *p*-toluenesulfonic acid, benzene, reflux, 5 min, 90%. j) *p*-benzoquinone or *p*-chloranil, benzene, reflux, 10 min. k) K-mirror, under vacuum, THF-d_8, -78 ˚C, 1 week. l) K-mirror, under vacuum, THF-d_8, -78 ˚C. m) 1eq. $(p\text{-}BrC_6H_4)_3N\ SbCl_6$, CH_2Cl_2. n) 2eq. $(p\text{-}BrC_6H_4)_3N\ SbCl_6$, CH_2Cl_2. o) conc. D_2SO_4 or excess $(p\text{-}BrC_6H_4)_3N\ SbCl_6$, CH_2Cl_2.

Scheme 1. Synthesis of **3•**, and six redox species.

tris(bromomethyl) compounds **7**, which were used for the next reaction without purification due to the instability. The reaction of **7** with diethyl malonate afforded hexakis(ethoxycarbonyl) derivatives **8**, which were converted to tris(propionic acids) **9** by hydrolysis and subsequent decarboxylation. The Friedel–Crafts cyclization of the acid chlorides obtained by the reaction of **8** with oxalyl chloride afforded triketone compounds **10** in 99% yield. The triketones **10** were reduced with lithium aluminum hydride, giving triols. Dehydration of the triols with a catalytic amount of *p*-toluenesulfonic acid afforded the compounds **11**. The target neutral monoradical species **3•** was obtained as an air-sensitive brown solid by the reaction of **11** with 1.5 equivalents of *p*-chloranil or *p*-benzoquinone.

The deuterated radical **12•** was also prepared following Scheme 2 in order to determine the hyperfine coupling constants (vide infra) of the radical species precisely.

Six redox states of **3•**: i.e. $\mathbf{3}^{3+}$, $\mathbf{3}^{\bullet 2+}$, $\mathbf{3}^{+}$, $\mathbf{3}^{-}$, $\mathbf{3}^{\bullet 2-}$, and $\mathbf{3}^{3-}$, were generated from the neutral species **3•**. The trianion $\mathbf{3}^{3-}$ was also obtained by the treatment of trihydro compounds **11** with a potassium mirror.

Properties of Neutral Radical 3•. Electrochemistry. The cyclic voltammogram of **3•** measured in CH_2Cl_2 exhibited six reversible one-electron redox waves ($E_3^{ox} = +0.87$ V, $E_2^{ox} = +0.68$ V, $E_1^{ox} = +0.27$ V, $E_1^{red} = -0.51$ V, $E_2^{red} = -0.89$ V, $E_3^{red} = -1.25$ V; $E_1^{sum} = 0.78$ V, $E_2^{sum} = 1.57$ V, $E_3^{sum} = 2.12$ V) as shown in Fig. 3. This observation provides evidence for the formation of the stable singly, doubly, and triply charged species. To our knowledge, only a few examples are known of compounds that exhibit six-stage amphoteric redox behavior.[4]

The sum of the redox potentials, E_1^{sum} of **3•** is substantially smaller than those reported thus far for hydrocarbons. Such a small E_1^{sum} value can be explained in terms of the electronic stability of three redox states of the phenalenyl units owing to

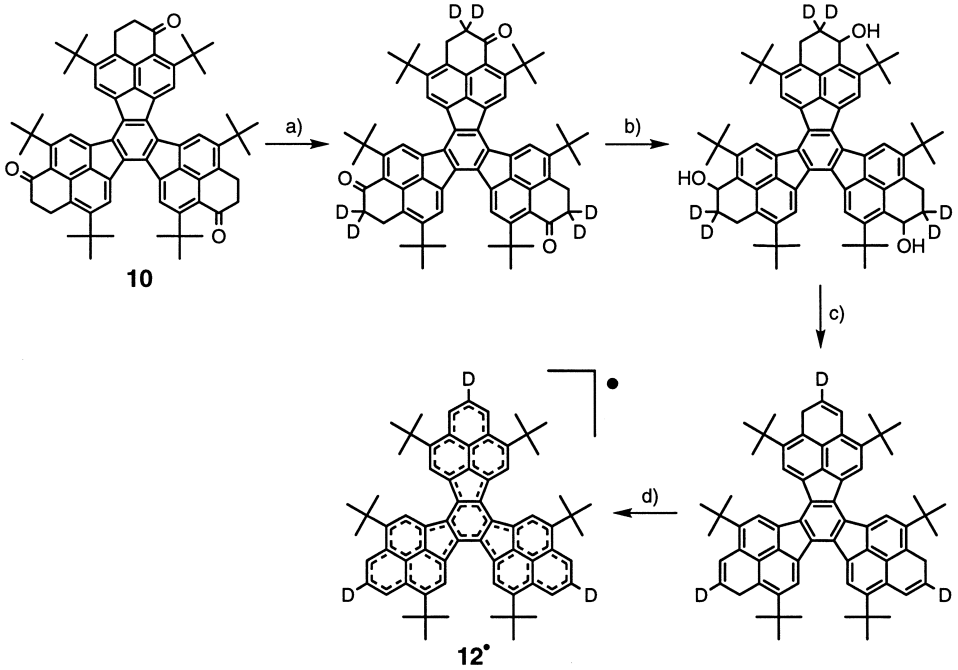

Reaction condition : a) CF_3COOD, CH_2Cl_2, 55 ˚C, 12 h, 100%. b) $LiAlH_4$, THF, rt, 2 h, 75%. c) *p*-toluenesulfonic acid, benzene, reflux, 5 min. d) *p*-chloranil, benzene, 60 ˚C, 15 min.

Scheme 2. Synthesis of the deuterated radical **12•**.

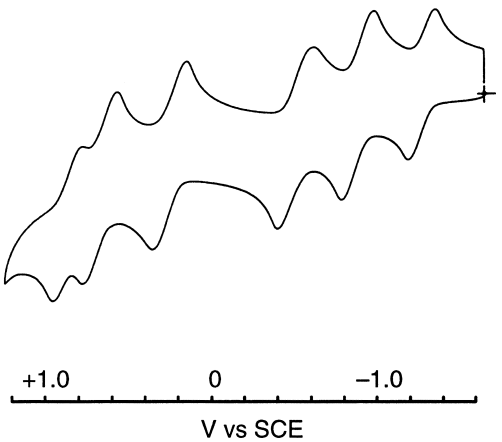

Fig. 3. Cyclic voltammogram (vs SCE) of **3•** in dichloromethane with 0.1 M $(^n Bu)_4NClO_4$ as supporting electrolyte at room temperature; sweep rate = 100 mv/s.

the delocalization of the generated charges or the unpaired electron over the molecule.

ESR Spectroscopy. Although numerous studies on free radicals have been reported, those on stable hydrocarbon radicals have been few. The representative examples are triphenylmethyl,[5] Kölsch's,[6] cyclopentadienyl,[7] and phenalenyl radical.[8] In particular, a simple alkyl derivative of the last example, tri-*t*-butylphenalenyl radical, gave single crystals; the crystal structure was determined at room temperature recently.[9] These hydrocarbons should be stabilized kinetically by steric hindrance and thermodynamically by spin delocalization.

The neutral hydrocarbon **3•** is also expected to be stable because of the steric hindrance by the bulky t-butyl groups and the highly delocalized structure. The dehydrogenation of the compounds **11** with *p*-benzoquinone or *p*-chloranil provided the neutral monoradical species as a brown solid. The neutral radical was unexpectedly found to decompose in a day on exposure to air.

The toluene solution of **3•** exhibited ESR spectrum too ill-resolved to determine the hyperfine coupling constants. However, the deuterated derivative **12•** gave an ESR spectrum with hyperfine structure, from which two coupling constants were obtained: 0.143 mT (6H), 0.047 mT (6H). The coupling con-

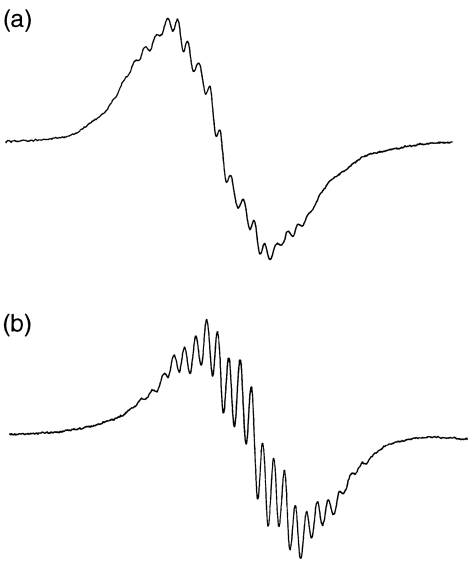

Fig. 4. ESR spectra of (a) **3•** and (b) **12•** at −30 °C in toluene.

Table 1. Experimental and Theoretical Hyperfine Coupling Constants (in mT) of **3**$^{\bullet}$, **3**$^{\bullet 2+}$, **3**$^{\bullet 2-}$, **12**$^{\bullet}$, **12**$^{\bullet 2+}$, and **12**$^{\bullet 2-}$

	3$^{\bullet}$ and **12**$^{\bullet}$ [a]		**3**$^{\bullet 2+}$ [b]		**3**$^{\bullet 2-}$ and **12**$^{\bullet 2-}$ [c]	
	Exptl	Theor[d]	Exptl	Theor[e]	Exptl	Theor
α^1	0.143	−0.144	0.186	−0.186	0.33	—[f]
β^1(H)	0.037	+0.032	0.037	+0.057	0.071	—[f]
β^1(D)	0.006	+0.005	—	+0.009	0.011	—[f]
β^2	0.047	+0.024	0.106	+0.033	0.107	—[f]

a) Recorded in toluene at −30 °C. The *g*-value was 2.0025. b) Recorded in CH_2Cl_2 at −30 °C. The *g*-value was 2.0024. c) Recorded in THF at −30 °C. The *g*-value was 2.0024. d) Calculated by the HMO–McLachlan method ($\lambda = 1.2$)[13] and the McConnell equation ($Q = -2.6$ mT).[14] e) Calculated by the HMO–McLachlan method ($\lambda = 1.2$) and the McConnell equation ($Q = -2.4$ mT). f) Could not be calculated by the HMO–McLachlan method because of the localization of the spin and the charges.

stants at β^1 position were determined by a computer simulation. Figure 4 shows these ESR spectra. The experimental and theoretical hyperfine coupling constants are given in Table 1. The agreement between the experimental and theoretical coupling constants indicates that the unpaired electron delocalization is not confined to one phenalenyl unit but is operative over the entire C_3 symmetric molecule. The highly delocalized structure is consistent with a single occupancy of the degenerated or nearly degenerate molecular orbitals.

The near degeneracy of ψ_{22}, ψ_{23}, and ψ_{24} leads to the potential quartet state of neutral **3**$^{\bullet}$. However, **3**$^{\bullet}$ in a benzene matrix gave no quartet signals. Apparently, there is no or a considerably small contribution of the structure **3a** to the ground state of **3**$^{\bullet}$ (Chart 2).

UV/Vis/NIR. Figure 5 shows the electronic spectra of **3**$^{\bullet}$ along with trication **3**$^{3+}$ and trianion **3**$^{3-}$, while Table 2 lists the wavelengths of the band maxima.

In order to assign the electronic bands to transitions between orbitals, MO calculations were performed by the INDO/S

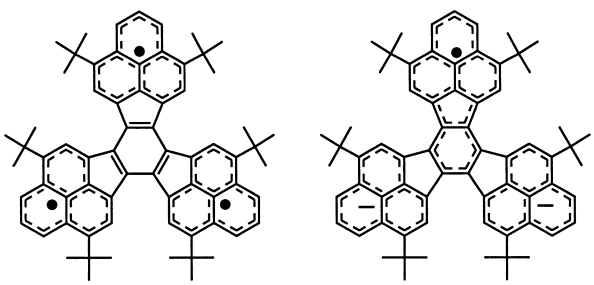

structure **3a** structure **3b**

Chart 2.

Table 2. Maxima, λ_{max} (in nm) (ε, cm^{-1} M^{-1}), of Electronic Bands for **3**$^{3+}$, **3**$^{\bullet}$, and **3**$^{3-}$

3^{3+}	**3**$^{\bullet}$	**3**$^{3-}$
231 (81800)	380	256 (39200)
494 (118000)	437	333 (34300)
550 (sh, 37900)	680	361 (37300)
601 (42500)	710	421 (21000)
676 (sh, 26700)	1130	507 (52300)
775 (sh, 7760)	1340	543 (56300)

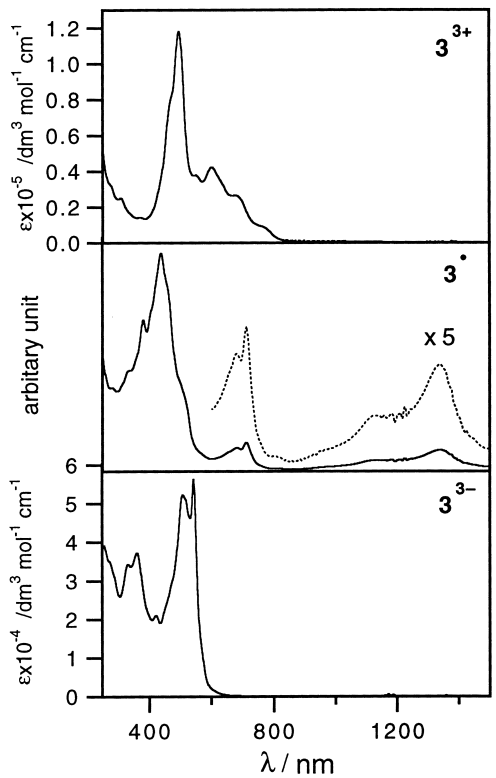

Fig. 5. Electronic spectra of **3**$^{3+}$, **3**$^{\bullet}$, and **3**$^{3-}$.

method (Table 3). In each case, the ten highest occupied and ten lowest unoccupied orbitals were used for configuration interaction. Figure 6 presents schematically the calculated SCF levels of seven relevant highest occupied and lowest unoccupied orbitals for **3**$^{\bullet}$, **3**$^{3+}$, and **3**$^{3-}$.

The many transitions in the visible region are responsible for the dark brown color of the **3**$^{\bullet}$. In addition to the low-energy band at 710 nm, **3**$^{\bullet}$ exhibited the weak and broad NIR transitions at 900–1500 nm. On the basis of the INDO/S calculation, these low-energy bands should be due to the transition in which SOMO participates. This calculation predicted the deviated C_2 structure for **3**$^{\bullet}$, where the degenerate *e* pair split into the SOMO *a* and the LUMO *b*. On the electronic transition time scale, the deviated C_2 structure might give the bands observed, while the time-averaged C_3 structure on ESR time

Table 3. Selected Electronic Transition Data for $\mathbf{3}^{3+}$, $\mathbf{3}^{\bullet}$, and $\mathbf{3}^{3-}$ Calculated by the INDO/S CI Method and Assignments of the Observed Electronic Bands

	Theoretical				Experimental
	Symmetry label	ΔE/eV	Oscillator strength	Substantial contribution/%	λ/nm; ΔE/eV
$\mathbf{3}^{3+}$		2.20	0.00	$e''(\psi_{101}) \leftarrow e''(\psi_{98})$, 28 $e''(\psi_{102}) \leftarrow e''(\psi_{99})$, 28 $a1''(\psi_{100}) \leftarrow a2''(\psi_{97})$, 18	a)
		2.33	0.08	$a1''(\psi_{100}) \leftarrow e''(\psi_{99})$, 40 $e''(\psi_{101}) \leftarrow e''(\psi_{99})$, 14 $e''(\psi_{102}) \leftarrow e''(\psi_{98})$, 14	a)
		2.33	0.08	$a1''(\psi_{100}) \leftarrow e''(\psi_{98})$, 40 $e''(\psi_{101}) \leftarrow e''(\psi_{98})$, 14 $e''(\psi_{102}) \leftarrow e''(\psi_{99})$, 14	a)
$\mathbf{3}^{\bullet}$	B	1.17	0.00	$b(\psi_{102})$[b] $\leftarrow a(\psi_{100})$, 64 $b(\psi_{102}) \leftarrow a(\psi_{101})$, 21	1340; 0.93
	A	1.42	0.02	$a(\psi_{101}) \leftarrow a(\psi_{100})$, 64 $a(\psi_{103}) \leftarrow a(\psi_{100})$, 14 $b(\psi_{102}) \leftarrow b(\psi_{99})$, 10	710; 1.75
$\mathbf{3}^{3-}$		2.53	0.00	$e''(\psi_{103}) \leftarrow e''(\psi_{102})$, 39 $e''(\psi_{104}) \leftarrow e''(\psi_{101})$, 39	c)
		2.63	0.00	$e''(\psi_{103}) \leftarrow e''(\psi_{101})$, 42 $e''(\psi_{104}) \leftarrow e''(\psi_{102})$, 42	c)
		2.67	1.41	$e''(\psi_{104}) \leftarrow a1''(\psi_{100})$, 21 $e''(\psi_{103}) \leftarrow e''(\psi_{101})$, 15 $e''(\psi_{104}) \leftarrow e''(\psi_{102})$, 15	543; 2.28
		2.67	1.41	$e''(\psi_{103}) \leftarrow a1''(\psi_{100})$, 21 $e''(\psi_{103}) \leftarrow e''(\psi_{102})$, 15 $e''(\psi_{104}) \leftarrow e''(\psi_{101})$, 15	543; 2.28

a) Could not be assigned due to the weak and broad peaks. b) The INDO/S calculations predicted the lower symmetry C_2 for $\mathbf{3}^{\bullet}$. In parentheses, the molecular orbitals calculated by the INDO/S method. See also Fig. 6. c) Could not be observed due to the intense band at 543 nm.

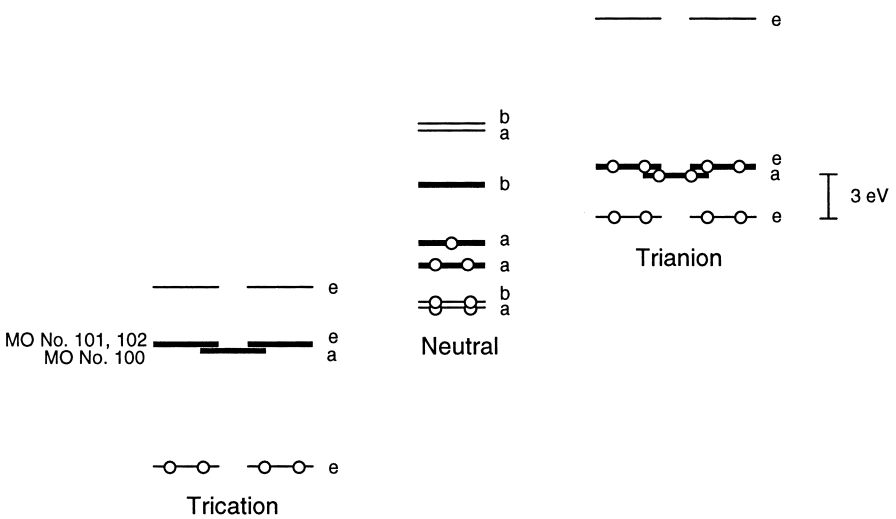

Fig. 6. Energy levels of several occupied and unoccupied MOs in $\mathbf{1}^{3+}$, $\mathbf{1}^{\bullet}$, and $\mathbf{1}^{3-}$, as calculated by the INDO/S method. The optimized structures are obtained by PM3 method, which gave a C_2 structure for neutral state and C_3 ones for other states. The bold lines represent HOMO, SOMO, and LUMO of neutral state.

scale might exhibit an ESR signal indicating the unpaired electron delocalization over the entire C_3 molecule.

Properties of Trication and Trianion. NMR spectroscopy: Trication $\mathbf{3}^{3+}$. Many polycyclic benzenoid hydrocarbons are known to generate dication species in super acids; these serve as oxidizing agents to remove electrons from molecules. In general, relatively small hydrocarbons tend to yield a mixture of radical cation and dication species, and to be proto-

Table 4. ^{1}H and ^{13}C NMR Data of $\mathbf{3}^{3+}$, and $\mathbf{3}^{3-}$

	α^1	α^2	α^3	β^1	β^2	3a, 7a 10a, 14a 17a, 21a	7b, 14b 21b	7c, 14c 21c	5b, 5c 12b, 12c 19b, 19c	$C(CH_3)_3$	$C(CH_3)_3$
$\mathbf{3}^{3+}$ a)	9.68			8.31	8.86						1.99
$\mathbf{3}^{3-}$ a)	7.97			7.50	9.49						2.00
$\mathbf{3}^{3+}$ b)	148.32	183.45	152.57	132.40	125.37	133.54	125.63	136.95	145.31	41.77	35.20
$\mathbf{3}^{3-}$ b)	113.40	126.98	114.27	118.63	120.10	130.75	129.58	127.62	119.03	37.16	32.55

a) ^{1}H NMR chemical shifts (δ). b) ^{13}C NMR chemical shifts (δ). $\mathbf{3}^{3+}$, recorded in D_2SO_4 at room temperature. $\mathbf{3}^{3-}$, recorded in THF-d_8 at room temperature.

nated in the presence of a proton source. In contrast to the small aromatic hydrocarbons, large aromatic systems generally yield dication species in strong acid media easily. For example, the dication of hexacene is obtained in concentrated H_2SO_4.[10] However, limited examples gave trication species even in such a strong medium.

The trication species $\mathbf{3}^{3+}$ was very easily obtained as a dark green solution by dissolving $\mathbf{3}^{\bullet}$ in concentrated D_2SO_4 or as dark green needles by treating $\mathbf{3}^{\bullet}$ with three equivalents of tris(4-bromophenyl)ammoniumyl hexachloroantimonate, which is a weak one-electron oxidizing reagent. The trication was so stable that it remained unchanged even at 60 °C. The ^{1}H and ^{13}C NMR chemical shifts are given in Table 4.

The simple ^{1}H and ^{13}C NMR spectra reflect the effective D_{3h} or C_3 structure of $\mathbf{3}^{3+}$. The ^{13}C chemical shifts of phenalenyl units in $\mathbf{3}^{3+}$ are found to be similar to those of phenalenyl cation except for α^2-carbons of $\mathbf{3}^{3+}$. The HMO calculations indicate that 90% of three positive charges reside on three phenalenyl units. These findings suggest that the positive charge is delocalized mainly over three phenalenyl units.

The ^{13}C NMR spectra of $\mathbf{3}^{3+}$ reveals only minor differences in chemical shifts compared to those of tetra-*t*-butyl IDPL dication $\mathbf{13}^{2+}$.[2g] In contrast to the similarity of ^{13}C chemical shifts, ring protons of $\mathbf{3}^{3+}$ appear in considerably lower field region than those of $\mathbf{13}^{2+}$. ^{1}H chemical shifts are well-known to be sensitive not only to charge but also to ring current. The London–McWeeny ring current calculations[11] as shown in Fig. 7 indicate that the smaller contributions of paramagnetic ring current effects, which is consistent with the larger HOMO (ψ_{20}, ψ_{21})–LUMO (ψ_{22}) gap of $\mathbf{3}^{3+}$, may be responsible for the lower-field shifts of $\mathbf{3}^{3+}$ in comparison with $\mathbf{13}^{2+}$.

NMR spectroscopy: Trianion $\mathbf{3}^{3-}$. The trianion $\mathbf{3}^{3-}$ was generated as a red purple solution by the reaction of the compounds **11** with a potassium mirror in a sealed degassed tube at −78 °C for a week. The trianion was found to be stable even at room temperature. The ^{1}H and ^{13}C NMR chemical shifts are given in Table 4.

Trianion also gave the simple ^{1}H and ^{13}C NMR spectra, indicating the effective D_{3h} or C_3 structure of $\mathbf{3}^{3-}$. The total ^{13}C chemical shift change of the sp^2 carbon atoms on going from $\mathbf{3}^{3+}$ and $\mathbf{3}^{3-}$ is 1041.63 ppm (or 173.61 ppm/e), which supports the idea of the existence of the trication and trianion, because the Spiesecke–Schneider correlation predicts a total ^{13}C chemical shift of 160–200 ppm per unit of charge.[12] The shift changes are large for the C atoms at α^1, α^2, and α^3, which correspond to the α-position of phenalenyl species, but small for the C atoms at other positions except for the central benzene ring. This finding indicates the large contribution of three phenalenyl units to the stability of $\mathbf{3}^{3+}$ and $\mathbf{3}^{3-}$.

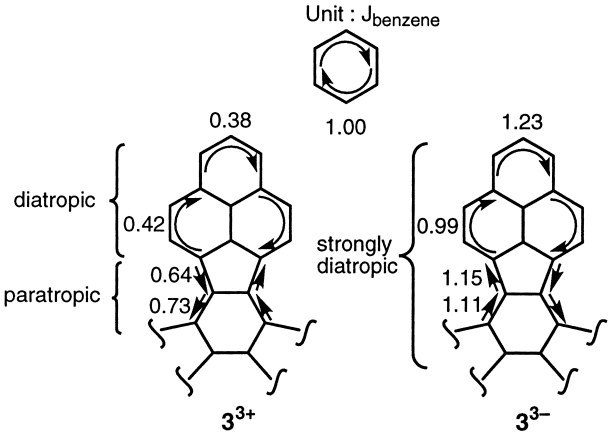

Fig. 7. Ring current calculation of $\mathbf{3}^{3+}$ and $\mathbf{3}^{3-}$.

The trianion $\mathbf{3}^{3-}$ also exhibited considerable downfield shifts of all ring protons, in spite of the shielding effect caused by the three negative charges. In particular, the signals of the protons at β^2-position of $\mathbf{3}^{3-}$ unexpectedly appear at lower field than the signals of the corresponding protons of $\mathbf{3}^{3+}$. The ring current calculations indicate the pronounced diamagnetic ring currents along the periphery of the molecules (Fig. 7). Thus the charge-induced upfield shift is compensated with the opposite influence of a diamagnetic ring current which is built up on trianion formation.

UV/Vis/NIR. The absorption spectra of $\mathbf{3}^{3+}$ essentially consist of weak and broad bands at 600–800 nm and a relatively intense band at 494 nm. The weak bands should be due to HOMO→LUMO and HOMO→NLUMO transitions. The INDO/S calculation predict the C_3 symmetry for $\mathbf{3}^{3+}$ and HOMO (ψ_{20} and ψ_{21}) and NLUMO (ψ_{23} and ψ_{24}) remains degenerate. The degeneracy of the orbitals may cause the participation of many transitions in a band.

A similar statement should hold for $\mathbf{3}^{3-}$. However, the predicted first and second bands were not observed due to the intense band at 543 nm. The intense band at 543 nm consists of many transitions in which NHOMO–LUMO and HOMO–NLUMO excitation participate in addition to the HOMO–LUMO transition. The absorption bands of $\mathbf{3}^{3-}$ terminate at the shortest wavelength region, which is consistent with a small paramagnetic ring current effect, i.e. a large diamagnetic effect in ^{1}H NMR spectrum as $\mathbf{13}^{2-}$

Properties of Monoradical Dication and Monoradical

Dianion. ESR Spectroscopy: Monoradical Dication $3^{\bullet 2+}$. Removal of two electrons from neutral $\mathbf{3}^{\bullet}$ should give the monoradical dication species $\mathbf{3}^{\bullet 2+}$. On the basis of the HMO calculations, the SOMO corresponds to non-degenerate molecular orbital ψ_{22}.

The monoradical dication $\mathbf{3}^{\bullet 2+}$ was obtained as dark green powder by the treatment of $\mathbf{3}^{\bullet}$ with two equivalents of $(p\text{-}BrC_6H_4)_3NSbCl_6$. Oxidation of $\mathbf{3}^{\bullet}$ with two equivalents of $SbCl_5$ also gave $\mathbf{3}^{\bullet 2+}$ as a dark green solution. The solution of $\mathbf{3}^{\bullet 2+}$ exhibited well-resolved ESR spectra, as shown in Fig. 8. Table 1 shows the hyperfine coupling constants of $3^{\bullet 2+}$.

The coupling constants of $\mathbf{3}^{\bullet 2+}$ are larger than those of $\mathbf{3}^{\bullet}$. This behavior is consistent with the HMO calculations indicating larger AO coefficients on the phenalenyl units in the non-degenerate orbital ψ_{22} (SOMO for $\mathbf{3}^{\bullet 2+}$) compared to the degenerate orbitals ψ_{23} and ψ_{24} (SOMO's for $\mathbf{3}^{\bullet}$). On the basis of the HMO–McLachlan calculations,[13] 98% of the π-spin population resides on the three phenalenyl units in $\mathbf{3}^{\bullet 2+}$, while these units of $\mathbf{3}^{\bullet}$ possess 84% of the total spin population. The well-resolved ESR signal also reflects the non-degeneracy of SOMO of $\mathbf{3}^{\bullet 2+}$.

ESR Spectroscopy: Monoradical Dianion $3^{\bullet 2-}$. The monoradical dianion $\mathbf{3}^{\bullet 2-}$ was generated by the reaction of $\mathbf{3}^{\bullet}$ with a potassium mirror in THF or DME. Further contact of the solution with a potassium mirror yielded trianion $\mathbf{3}^{3-}$. The pair of the relevant frontier orbitals is degenerate or nearly degenerate with an occupancy number of three in $\mathbf{3}^{\bullet 2-}$.

The ESR spectra of $\mathbf{3}^{\bullet 2-}$ and $\mathbf{12}^{\bullet 2-}$ were given in Fig. 9. A similar spectrum was observed on the oxidation of $\mathbf{3}^{3-}$ with $(p\text{-}BrC_6H_4)_3NSbCl_5$. The ESR studies for the monoradical dianion species reveal that the unpaired electron is "localized" mainly on one phenalenyl unit. The localized structure can be investigated by simply counting the number of equivalent protons giving rise to a particular coupling constants. Simulation of the experimental ESR spectra gives the following coupling: 0.330 mT (2H), 0.107 mT (2H), and 0.071 mT (1H). The coupling constants were assigned as shown in Table 2 but the assignment still remains questionable, because we could not calculate the spin density of $\mathbf{3}^{\bullet 2-}$ in such a localized structure by the use of the HMO–McLachlan method. The smaller coupling constants of $\mathbf{3}^{\bullet 2-}$ compared to phenalenyl radical suggest that the unpaired electron resides not only on one phenalenyl unit but also on the central benzene unit. Thus formula **3b** is the best description for monoradical dianion species $\mathbf{3}^{\bullet 2-}$.

The unpaired electrons of $\mathbf{13}^{\bullet -}$ are delocalized over the entire molecule, while $\mathbf{3}^{\bullet 2-}$ has a localized structure.[15] The followings are our way of finding the reason for some aspects of

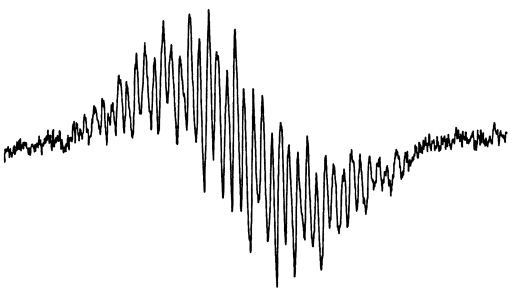

Fig. 8. ESR spectrum of $\mathbf{3}^{\bullet 2+}$ at -30 °C in CH_2Cl_2.

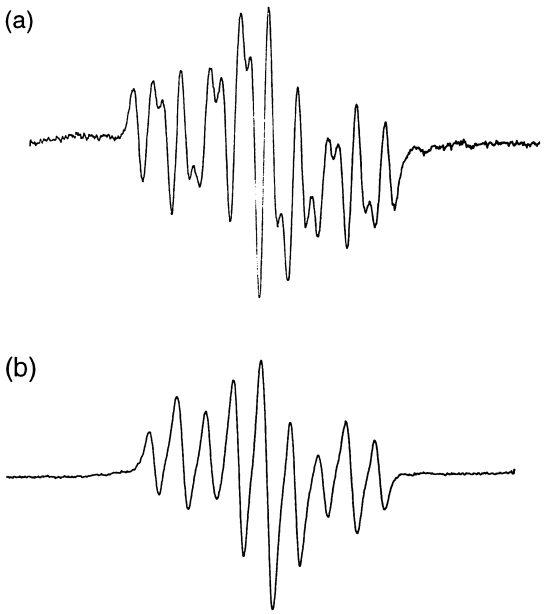

Fig. 9. ESR spectra of (a) the dianion monoradical $\mathbf{3}^{\bullet 2-}$ and (b) the deuterated derivative $\mathbf{12}^{\bullet 2-}$ at -30 °C in THF.

behavior observed.

In general, a compound with partially filled degenerate orbitals is unstable to vibrational modes to break down the high symmetry of the molecule in question, and is subject to the Jahn–Teller distortion to a lower symmetry structure. For $\mathbf{3}^{\bullet 2-}$, two counter cations K^+ will reside near two phenalenyl units and may allow the localization of two negative charges in two phenalenyl units. In solvents such as THF, which favor the formation of contact ion pairs, $\mathbf{3}^{\bullet 2-}$ should possess a distorted structure with spin and negative charges-localization. However, even under such conditions as a solvent-separated ion pair, i.e. DME at low temperature (-30–-80 °C) or 18-crown-6 in THF, the ESR spectrum observed was consistent with the localized structure. In such conditions, ion pairing may contribute limitedly to localization in $\mathbf{3}^{\bullet 2-}$.[16]

Properties of Monocation. Removal of one electron from the neutral radical $\mathbf{3}^{\bullet}$ should give the closed shell monocation $\mathbf{3}^{+}$. The treatment of $\mathbf{3}^{\bullet}$ with one electron oxidizing reagents, e.g. Ph_3CBF_4, Ph_3CSbCl_6, $(p\text{-}BrC_6H_4)_3NSbCl_6$, I_2, and $AlCl_3$, afforded dark green powder, which can be assigned to a monocation species. However, the solution of the dark green powder in CD_2Cl_2 at room temperature gave no signals except for a considerably broad peak at 1–2 ppm. The change of solvents (CD_2Cl_2 + CF_3COOD, CD_2Cl_2 + CD_3COOD, or acetone-d_6) and temperatures (30 °C–-80 °C) did not affect the shape of the peak. The broad peak is attributable to the equilibrium between the paramagnetic species and $\mathbf{3}^{+}$. The following three mechanisms seem plausible for the equilibrium:

1) Disproportionation
$$\mathbf{3}^{+} \rightleftarrows \mathbf{3}^{\bullet} + \mathbf{3}^{\bullet 2+}$$
2) Electron transfer
$$\mathbf{3}^{\bullet} + \mathbf{3}^{\bullet 2+} \rightleftarrows \mathbf{3}^{\bullet 2+} + \mathbf{3}^{\bullet}$$
3) Electron transfer via other component **X**
$$\mathbf{3}^{+} + \mathbf{X} \rightleftarrows \mathbf{3}^{\bullet} + \mathbf{X}^{\bullet +}$$

Some observations provide some insight. A trace of paramagnetic species were detected by ESR measurement of the

solution of the dark green powder. The ESR spectrum was identical with that of $\mathbf{3}^{\bullet 2+}$ and the signal intensity was independent of temperatures. These findings make the disproportionation mechanism seem unlikely. Thus the electron transfer between $\mathbf{3}^{+}$ and a trace of $\mathbf{3}^{\bullet 2+}$ will be responsible for the broad signal. Elemental analysis for the dark green powder also supports the presence of $\mathbf{3}^{\bullet 2+}$.[17]

Dissolution of the green powder in D_2SO_4 exhibited the simple pattern of ^{1}H NMR spectrum, which is identical with that of $\mathbf{3}^{3+}$. This excludes the possibility of the decomposition of the basic structure. At present, several attempted isolations of the pure $\mathbf{3}^{+}$ failed.

Properties of Monoanion. The prime interest about $\mathbf{3}^{-}$ relates to whether this species will be singlet or triplet. The potential triplet state can be understood from the simple molecular orbital energy pattern derived from HMO calculations, providing ideas that a degenerate pair of orbitals (ψ_{23} and ψ_{24}) is half occupied and that the electrons can occupy separated orbitals with unpaired spins.

On exposure of a DME solution of $\mathbf{3}^{\bullet}$ to a potassium mirror, the intensity of the ESR signal of $\mathbf{3}^{\bullet}$ gradually decreased, and finally the signal became a small and broad peak. At this stage, we measured the ESR spectrum of the rigid solution of the reduced species at 77 K and 173 K, but no triplet signals were observed. Further reduction produced a new broad signal, which finally became a moderately-resolved ESR peak identical with those of $\mathbf{3}^{\bullet 2-}$. More advanced calculation (PM3) predicted a triplet ground state (total energy: -5653.11 eV) rather than a singlet one (-5651.77 eV) and the charge delocalization over the entire molecule. However, the ion pair of K^+ with one phenalenyl unit may cause the negative charge localization, which will lead to a singlet ground state suggested by the absence of the triplet ESR signal.

Conclusion. The hydrocarbon radical $\mathbf{3}^{\bullet}$ containing three phenalenyl units was found to exhibit high amphotericity and to behave as a six-stage amphoteric redox compound. This means that one molecule has as many as seven electronic states. The single crystal of the neutral radical could not be obtained, but $\mathbf{3}^{\bullet}$ was stable enough to isolate and we could study the properties. The highly delocalized structure and bulky *t*-butyl groups should stabilize $\mathbf{3}^{\bullet}$ thermodynamically and kinetically. Surprisingly, $\mathbf{3}^{\bullet}$ gave super-charged species, i.e. trication and trianion, with no difficulties.

The basic π-electronic structure of redox states of $\mathbf{3}^{\bullet}$ was essentially similar to the structure of those of **13**, while the most remarkable differences were found in $\mathbf{3}^{\bullet 2-}$, which exhibited spin localization on one phenalenyl unit. These differences would be caused by the Jahn–Teller effect. The orbital degeneracy made some differences in the properties of the redox states between $\mathbf{3}^{\bullet}$ and **13**.

Experimental

Material and Methods. All experiments with moisture- or air-sensitive compounds were performed in anhydrous solvents under an argon atmosphere in flame-dried glassware. Solvents were dried and distilled according to the standard procedures. Column chromatography were performed with silica gel [Wako gel C-200 (Wako)] or basic alumina [200 mesh (Wako)]. Infrared spectra were recorded on a Perkin Elmer FT 1640 IR spectrometer. Electronic spectra were measured by a Shimadzu UV-3100PC spectrometer. ^{1}H and ^{13}C NMR spectra were obtained on JEOL EX-270, JEOL GSX-400, JEOL GSX-500, and Varian UNITY plus 600 spectrometers. Positive FD mass spectra were taken by using JEOL JMS SX-102 and Shimadzu QP-5000 mass spectrometers. ESR spectra were obtained with a JEOL JES-FE2XG spectrometer. Cyclic voltammetric measurements were made with a Yanagimoto P1100 spectrometer. Cyclic voltammograms of the compounds were recorded with a glassy carbon working electrode and a Pt counter electrode in CH_2Cl_2 containing 0.1 M $(n\text{-Bu})_4NClO_4$ as the supporting electrolyte. The experiments employed a SCE reference electrode. Electrochemical experiments were done under a argon atmosphere at room temperature.

2,5,8,11,14,17-Hexa-*t*-butyldecacyclene (4). To a suspension of decacyclene (Aldrich; 5.64 g, 12.5 mmol) in CH_2Cl_2 (300 mL) were added *t*-butyl chloride (28 mL) and anhydrous $AlCl_3$ (2.1 g, 15.7 mmol) at room temperature and this mixture was stirred for 1 h. Additional *t*-butyl chloride (10 mL) was added and the reaction mixture was stirred for 1 h. The mixture was poured into ice-water and the organic layer was separated. The aqueous layer was extracted repeatedly with small portions of CH_2Cl_2. The combined organic layers were dried over Na_2SO_4 and filtered, and the solvent was removed. Pure **4** (7.3 g, 74%) was obtained after column chromatography on silica gel [benzene/hexane (1:10, v/v)] and subsequent recrystallization (ethanol + CH_2Cl_2). m.p. $>$ 300 °C. ^{1}H NMR (270 MHz, $CDCl_3$) δ 8.97 (d, J = 1 Hz, 6H), 7.92 (d, J = 1 Hz, 6H), 1.66 (s, 54H). ^{13}C NMR (67.8 MHz, $CDCl_3$) δ 151.05, 137.09, 136.44, 131.45, 129.65, 122.19, 121.83, 35.85 [*C*$(CH_3)_3$], 32.02 [C(*C*$H_3)_3$]. FD MS *m/z*: 786 (M^+). Anal. Found: C, 91.38; H, 8.43%. Calcd for $C_{60}H_{66}$: C, 91.55; H, 8.45%.

2,5,8,11,14,17-Hexa-*t*-butyl-1,6,12/13-tribromodecacyclene (5). Compound **4** (7.87 g, 10 mmol) was dissolved in CH_2Cl_2 (300 mL) and bromine (1.6 mL, 31.1 mmol) was added to the solution; this mixture was stirred for 6 h at room temperature. Ten-percent aqueous sodium thiosulfate solution was added to the reaction mixture to reduce the excess bromine. The organic layer was separated and the aqueous layer was extracted with CH_2Cl_2. The combined organic layer were dried over Na_2SO_4 and filtered, and then the solvent was removed. The crude product was purified by column chromatography on silica gel [benzene/hexane (1:10, v/v)] to give **5** (7.8 g, 76%). ^{1}H NMR (270 MHz, $CDCl_3$) δ 8.88–8.86 (3H), 8.78–8.74 (3H), 8.43–8.38 (3H), 1.88–1.63 (54H). FD MS *m/z* 1020 (M^+).

2,5,8,11,14,17-Hexa-*t*-butyl-1,6,12/13-trimethyldecacyclene (6). Butyllithium (7.3 mL, 11.7 mmol, 1.6 M in hexane) was added to a solution of **5** (2.0 g, 1.95 mmol) in 150 mL of THF at -78 °C. After stirring for 15 min, methyl iodide (1.46 mL, 23.4 mmol) was added. The reaction mixture was allowed to warm to room temperature over night. Saturated aqueous ammonium chloride solution and 100 mL of benzene were added to the reaction mixture. The organic layer was separated and the aqueous layer was extracted repeatedly with small portions of benzene. The combined organic layers were dried over Na_2SO_4 and filtered. After evaporation of the solvent, purification by column chromatography on silica gel [benzene/hexane (1:4, v/v)] followed by recrystallization (CH_2Cl_2 + ethanol) gave pure **6** (1.31 g, 81%). ^{1}H NMR (270 MHz, $CDCl_3$) δ 8.89–8.87 (3H), 8.82–8.79 (3H), 8.13–8.12 (3H), 3.08–3.07 (9H), 1.76–1.62 (54H). FD MS *m/z* 828 (M^+).

2,5,8,11,14,17-Hexa-*t*-butyl-1,6,12/13-tris(bromomethyl)decacyclene (7). The mixture of compound **6** (829 mg, 1 mmol),

N-bromosuccinimide (587 mg, 3.3 mmol), benzoyl peroxide (80 mg, 0.33 mmol) in 100 mL of benzene were refluxed for 20 min. The reaction mixture was concentrated in vacuo and 3 mL of hexane was added. The resulting colorless precipitate was removed by filtration and the filtrate was concentrated in vacuo to give crude **7** (1.02 g, 95.5%). ^{1}H NMR (270 MHz, $CDCl_3$) δ 8.85–8.80 (3H), 8.75–8.69 (3H), 8.34–8.33 (3H), 5.54–5.52 (6H), 1.81–1.64 (54H).

2,5,8,11,14,17-Hexa-*t*-butyl-1,6,12/13-tris[2,2-bis(ethoxycarbonyl)ethyl]decacyclene (8). Diethyl malonate (0.91 mL, 6.03 mmol) was added to a sodium ethoxide solution freshly prepared from 15 mL of anhydrous ethanol and sodium (126 mg, 5.48 mmol). To the clear solution was added **7** (1.02 g, 0.955 mmol) dissolved in benzene (15 mL). After stirring for 4 h, the reaction mixture was washed with water. The organic layer was separated and the aqueous layer was extracted repeatedly with small amounts of benzene. The combined organic layers were dried over $MgSO_4$ and filtered. After evaporation of the solvent, the crude product was purified by column chromatography on silica gel (benzene) to give **8** (383 mg, 31%). ^{1}H NMR (270 MHz, $CDCl_3$) δ 8.88 (s, 3H), 8.80 (s, 3H), 8.03–8.02 (3H), 4.28 (m, 6H), 4.22–3.92 (m, 12H), 3.91 (m, 3H), 1.74–1.61 (54H), 1.13–1.05 (18H). FD MS *m/z* 1303 (M^+).

2,5,8,11,14,17-Hexa-*t*-butyl-1,6,12/13-tris(2-carboxyethyl)decacyclene (9). A suspension of **8** (383 mg) in ethanol (14 mL) and 10% aqueous potassium hydroxide solution (7 mL) was refluxed for 3 h. The reaction mixture was cooled and concentrated in vacuo. The obtained yellow solid in 4 M hydrochloric acid (20 mL) was heated with refluxing for 8 h. The resulting yellow precipitate was collected and washed with water. Pure **9** (280 mg, 95%) was obtained after column chromatography on silica gel [benzene/acetone (3:1, v/v)]. FD MS *m/z* 1003 (M^++H). IR (KBr) 3600–2500, 2961, 1709 cm^{-1}.

4,7,11,14,18,21-Hexa-*t*-butyl-2,3,8,9,10,15,16,17-octahydro-1,8,15/17-trioxo-1*H*-tribenzodecacyclene (10). A mixture of compound **9** (500 mg, 0.498 mmol) and oxalyl chloride (3 mL) was heated with refluxing for 1 h. The reaction mixture was cooled and concentrated in vacuo. The resulting orange solid was dissolved in CH_2Cl_2 (70 mL) and cooled to -78 °C. Anhydrous $AlCl_3$ (750 mg, 5.62 mmol) was added to the solution and the reaction mixture was allowed to warm to -50 °C over 2 h, and stirred at -50 °C for 4 h. To the mixture was added 2 M hydrochloric acid and the organic layer was separated. The aqueous layer was extracted with small portion of CH_2Cl_2. The combined organic layers were washed with brine and dried over Na_2SO_4 and filtered. After column chromatography on silica gel (CH_2Cl_2), pure **10** (467 mg, 98.8%) was obtained as an orange powder. ^{1}H NMR (270 MHz, $CDCl_3$) δ 8.99–8.95 (3H), 8.85–8.80 (3H), 3.91 (t, 6H), 3.23 (t, 6H), 1.73–1.70 (54H). FD MS *m/z* 949 (M^++H). IR (KBr) 2965, 1699 cm^{-1}.

4,7,11,14,18,21-Hexa-*t*-butyl-8,15/17-dihydro-1*H*-tribenzodecacyclene (11). 1) A mixture of **10** (467 mg, 12.2 mmol) and $NaBH_4$ (460 mg, 12.2 mmol) in CH_2Cl_2 (20 mL) and ethanol (10 mL) was refluxed for 24 h. The mixture was cooled and 2 M hydrochloric acid was added dropwise. The organic layer was separated and the aqueous layer was extracted repeatedly with small portions of CH_2Cl_2. The combined organic layers were washed with brine and dried over Na_2SO_4, and filtered. After column chromatography on silica gel (CH_2Cl_2), pure triols (430 mg, 91.5%) was obtained as a yellow powder. ^{1}H NMR (270 MHz, $CDCl_3$) δ 8.78 (s, 6H), 5.90 (br, 3H), 3.71 (m, 3H), 3.48 (m, 3H), 2.59 (m, 3H), 2.17 (m, 3H), 1.76–1.71 (54H). FD MS *m/z* 955 (M^+), 937 (M^+-H_2O), 919 (M^+-2H_2O), 901 (M^+-3H_2O). IR (KBr) 3425, 2956 cm^{-1}.

2) Triols (57 mg, 59.7 µmol) in benzene (15 mL) were heated with refluxing. *p*-Toluenesulfonic acid monohydrate (1 mg, 5.2 µmol) was added to the solution, and the reaction mixture was stirred for 5 min. The mixture was cooled rapidly on an ice-bath and concentrated at room temperature in vacuo. The crude product was purified by column chromatography on silica gel [benzene/hexane (1:4, v/v)] to give **11** (39.8 mg, 74%). ^{1}H NMR (270 MHz, $CDCl_3$) δ 8.95 (s, 3H), 8.88 (s, 3H), 7.66 (dt, J = 10.56, 1.97 Hz, 3H), 6.61 (dt, J = 10.56, 4.29 Hz, 3H), 4.31 (dd, J = 1.97, 4.29Hz, 3H), 1.77 (54H). FD MS *m/z* 900 (M^+), 899 (M^+-H), 898 (M^+-2H), 897 (M^+-3H).

Deuterated Derivatives of 11. A solution of **10** (215 mg, 226 µmol) in CF_3COOD (2mL) was heated at 55 °C for 22 h. After cooling, the mixture was extracted with benzene, and the benzene solution was washed with saturated aqueous $NaHCO_3$, then with brine, dried over Na_2SO_4 and filtered. Purification with column chromatography on silica gel [benzene/ether (100:1, v/v)] gave deuterated **10** (163 mg, 76%). The same procedures as non-deuterated compounds afforded deuterated **11** (%D > 98%).

4,7,11,14,18,21-Hexa-*t*-butyltribenzodecacyclenyl Radical (3$^\bullet$). A mixture of **11** (41.5 mg, 46 µmol) and *p*-benzoquinone (12.4 mg, 115 µmol) in benzene (10 mL) was refluxed for 5 min. The mixture was cooled on an ice-bath and 40 mL of hexane was added to the mixture. The crude product was purified by column chromatography on silica gel [benzene/hexane (1:4, v/v)] to give **3**$^\bullet$ (22.4 mg, 54%). FD MS *m/z* 897 (M^+).

4,7,11,14,18,21-Hexa-*t*-butyltribenzodecacyclenyl Trication (3^{3+}). A mixture of **11** (53 mg, 58.8 µmol) and *p*-benzoquinone (9.5 mg, 88.2 µmol) in benzene (10 mL) was refluxed for 10 min. The mixture was cooled on an ice-bath and concentrated in vacuo. Hexane (20 mL) was added to the mixture and undissolved materials were removed by filtration. The crude **3**$^\bullet$ was dissolved in 5 mL of CH_2Cl_2 and cooled on an ice-bath. Tris(*p*-bromophenyl)ammoniumyl hexachloroantimonate (142 mg, 174 µmol) was added to the solution and the reaction mixture was stirred for 7 h. The dark green precipitates were removed by filtration and 6 mL of hexane was added to the filtrate. The mixture was cooled at 0 °C and allowed to stand at the same temperature overnight. The resulting dark green powder was collected, washed with hexane–CH_2Cl_2 (3:1) four times, and dried. Yield 58.1 mg (52%). Anal. Found: C, 43.06; H, 3.60%. Calcd for $C_{69}H_{69}Cl_{18}Sb_3$: C, 43.58; H, 3.66%.

4,7,11,14,18,21-Hexa-*t*-butyltribenzodecacyclenyl Radical Dication (3$^{\bullet 2+}$). A mixture of **3**$^\bullet$ (22.4 mg, 24.9 µmol) and tris(*p*-bromophenyl)ammoniumyl hexachloroantimonate (40.7 mg, 49.8 µmol) in 2 mL of CH_2Cl_2 was stirred at 0 °C for 2 h. Ether (6 mL) was added to the mixture with portions; this was allowed to stand at the same temperature overnight. The resulting dark green powder was filtered, washed with 2 mL of ether, and dried. Yield 10 mg (26%). Anal. Found: C, 53.09; H, 4.30%. Calcd for $C_{69}H_{69}Cl_{12}Sb_2$: C, 52.88; H, 4.44%.

4,7,11,14,18,21-Hexa-*t*-butyltribenzodecacyclenyl Monoanion and Radical Dianion (3$^-$ and 3$^{\bullet 2-}$). The anions were generated in a sealed degassed cell by the reaction of **3**$^\bullet$ with a K-mirror in THF or DME.

4,7,11,14,18,21-Hexa-*t*-butyltribenzodecacyclenyl Trianion (3^{3-}). The reaction of trihydro compounds **11** (7 mg, 7.8 µmol) with a potassium mirror in THF-d_8 (0.5 mL) in a sealed degassed tube afforded the trianion species. Trianion was also obtained by the reaction of **3**$^\bullet$ with a potassium mirror in THF in a sealed de-

gassed tube.

ESR Spectroscopy. Neutral 3•. *p*-Chloranil (1 mg, 4 μmol) was placed in the ESR tube and 1 mL of the toluene solution of **11** (10^{-4} M) was added by a syringe. The cell was connected to a vacuum line and the solution was degassed by a repeated freeze-pump-thaw method (5 times). The cell was sealed and heated at 60 °C for 5 min. The ESR spectra of **3•** were recorded in the range of −60 to 20 °C.

Radical Dication $3^{\bullet 2+}$. A solution of $3^{\bullet 2+}$ (3.3×10^{-4} M, 0.2 mL) in CH_2Cl_2 was introduced into the cell by a syringe. The cell was connected to a vacuum line and the solvent was degassed by a repeated freeze-pump-thaw method (5 times). The cell was sealed and the ESR spectra of radical dication were recorded at −30 °C.

Radical Dianion $3^{\bullet 2-}$. A clean piece of potassium was passed into the side arm connected with a cell and sealed. A solution of **3•** (1×10^{-3} M, 0.2 mL) in DME was introduced into the cell by a syringe. The cell was connected to a vacuum line and then the solvent was degassed by a repeated freeze-pump-thaw method (5 times). The side arm was warmed with a luminous flame to distill the metal as a mirror onto the walls. The side arm was removed by sealing. Finally, the cell was sealed. The contact of the solution with a potassium mirror at room temperature gave the radical dianion. The ESR spectra of radical dianion were recorded at −30–−80 °C.

Monoanion 3^-. The contact of a DME solution of **3•** (10^{-3} M) with a K-mirror exhibited the gradual decrease of signals of **3•** and a new broad signal appeared. At this stage, the solution was frozen at −100 °C and the ESR spectrum was measured. However, no triplet signal was observed. Prolonged contact with a K-mirror gave the moderately-resolved ESR spectrum attributable to $3^{\bullet 2+}$.

UV/Vis/NIR Spectroscopy. Trication 3^{3+}. The quantitative electronic spectrum of 3^{3+} was obtained by the dissolution of the 3^{3+} $(SbCl_6)_3$ (1.084 mg, 0.570 μmol) in D_2SO_4 (100 mL) at room temperature.

Neutral 3•. The compound **3•** was purified by column chromatography (silica gel). The pure **3•** was dissolved in cyclohexane and qualitative measurements were carried out at room temperature.

Trianion 3^{3-}. The contact of the THF solution of **11** (3.517×10^{-5} M) with a K-mirror at room temperature gave a red-purple solution. The ε-value was estimated assuming quantitative conversion of **11** to 3^{3-}.

References

1 A preliminary account of a part of this work; T. Kubo, K. Yamamoto, K. Nakasuji, T. Takui, and I. Murata, *Angew. Chem., Int. Ed. Engl.*, **35**, 439 (1996).

2 a) B. Hagenbruch, K. Hesse, S. Hünig, and G. Klug, *Justus Liebigs Ann. Chem.*, **1981**, 256. b) S. Hünig, M. Hornaer, and P. Schilling, *Angew. Chem., Int. Ed. Engl.*, **14**, 556 (1975). c) K. Nakasuji, K. Yoshida, and I. Murata, *J. Am. Chem. Soc.*, **104**, 1432 (1982). d) K. Nakasuji, K. Yoshida, and I. Murata, *Chem. Lett.*, **1982**, 969. e) K. Nakasuji, K. Yoshida, and I. Murata, *J. Am. Chem. Soc.*, **105**, 5136 (1983). f) I. Murata, S. Sasaki, K.-U. Klabunde, J. Toyoda, and K. Nakasuji, *Angew. Chem., Int. Ed. Engl.*, **30**, 172 (1991). g) K. Ohashi, T. Kubo, T. Masui, K. Yamamoto, K. Nakasuji, T. Takui, Y. Kai, and I. Murata, *J. Am. Chem. Soc.*, **120**, 2018 (1998). See also, V. D. Parker, *J. Am. Chem. Soc.*, **98**, 98 (1976); K. Deuchert and S. Hünig, *Angew. Chem., Int. Ed. Engl.*, **17**, 875 (1978); K. Takahashi and T. Suzuki, *J. Am. Chem. Soc.*, **111**, 5483 (1989); K. Takahashi, *Pure. Appl. Chem.*, **65**, 127 (1993); R. Bachmann, F. Gerson, G. Gescheidt, and E. Vogel, *J. Am. Chem. Soc.*, **114**, 10855 (1992); R. Bachmann, F. Gerson, G. Gescheidt, and E. Vogel, *J. Am. Chem. Soc.*, **115**, 10286 (1993); E. Vogel, J. Dörr, A. Herrmann, J. Lex, H. Schmickler, P. Walgenbach, J. P. Gisselbrecht, and M. Gross, *Angew. Chem., Int. Ed. Engl.*, **32**, 1597 (1993).

3 K. Nakasuji, M. Yamaguchi, I. Murata, K. Yamaguchi, T. Fueno, H. Ohya-Nishiguchi, T. Sugano, and M. Kinoshita, *J. Am. Chem. Soc.*, **111**, 9265 (1989).

4 J. Heinze, *Angew. Chem., Int. Ed. Engl.*, **20**, 202 (1981).

5 M. Gomberg, *J. Am. Chem. Soc.*, **22**, 757 (1900); *Ber. Dtsch. Chem. Ges.*, **33**, 3150 (1900); B. Kahr, D. V. Engen, and P. Gopalan, *Chem. Mater.*, **5**, 729 (1993).

6 C. F. Kölsch, *J. Am. Chem. Soc.*, **79**, 4439 (1957).

7 K. Ziegler and B. Schnell, *Justus Liebigs Ann. Chem.*, **445**, 266 (1925); H. Sitzmann, H. Bock, R. Boese, T. Dezember, Z. Havlas, W. Kaim, M. Moscherosch, and L. Zanathy, *J. Am. Chem. Soc.*, **115**, 12003 (1993).

8 D. H. Reid, *Chem. Ind. (London)*, **1956**, 1504.

9 K. Goto, T. Kubo, K. Yamamoto, K. Nakasuji, K. Sato, D. Shiomi, T. Takui, M. Kubota, T. Kobayashi, K Yakusi, and J. Ouyang, *J. Am. Chem. Soc.*, **121**, 1619 (1999); K. Fukui, K. Sato, D. Shiomi, T. Takui, K. Itoh, K. Goto, T. Kubo, K. Yamamoto, K. Nakasuji, and A. Naito, *Synth. Met.*, **103**, 2257 (1999).

10 H. Angliker, E. Rommel, and J. Wirz, *Chem. Phys. Lett.*, **87**, 208 (1982).

11 F. London, *J. Phys. Radium*, **8**, 397(1937). J. A. Pople, *Mol. Phys.*, **1**, 175 (1958). R. McWeeny, *Mol. Phys.*, **1**, 311 (1958). R. B. Mallion, *Mol. Phys.*, **25**, 1415 (1973). J. Aihara, *Bull. Chem. Soc. Jpn.*, **58**, 1045 (1985).

12 H. Spiesecke and W. G. Schneider, *Tetrahedron Lett.*, **1961**, 468.

13 A. D. McLachlan, *Mol. Phys.*, **3**, 233 (1960).

14 H. M. McConnell, *J. Chem. Phys.*, **24**, 764 (1956).

15 For localization vs. delocalization, see; S. Utamapanya and A. Rajca, *J. Am. Chem. Soc.*, **113**, 9242 (1991).

16 For electrostatic perturbation of counter cations, see; A. H. Reddoch, *J. Chem. Phys.*, **43**, 225 (1965).

17 Anal. Found: C 64.66, H 5.27%. Calcd for $C_{69}H_{69}(SbCl_6)_n$, $n = 1.0$: C 66.41, H 5.57%; $n = 1.15$, C 64.60, H 5.42%.